# Hall-Effect Measurements of the Double-Layer Capacitance of the Graphene-Electrolyte Interface

*Morgan A. Brown*[1,=], *Michael S. Crosser*[2,=], *Agatha C. Ulibarri*[2], *Carly V. Fengel*[1], *Ethan D. Minot*[1,*]

[1] *Department of Physics, Oregon State University, Corvallis, OR*

[2] *Department of Physics, Linfield College, McMinnville, OR*

[=] these authors contributed equally

*Corresponding Author E-mail Address ethan.minot@oregonstate.edu

**Abstract**

There is an ongoing effort to improve the energy storage capacity of graphene-based supercapacitors. These supercapacitors store energy in the electric field between the charge carriers in the graphene and the counter ions in a liquid electrolyte. To characterize this double-layer, we use the Hall effect to determine the charge carrier density in graphene as a function of voltage. We disentangle the separate roles of double-layer capacitance (the electrostatic contribution) and quantum capacitance, and compare the performance of different electrolytes. Our results highlight the advantages of Hall-effect measurements for probing the electrostatics of graphene-electrolyte interfaces.

## Introduction

Supercapacitor devices play an increasingly important role in energy management, offering benefits such as fast charging/discharging rates and long lifetime.[1,2] At the heart of a supercapacitor (also known as an electrochemical capacitor) is the solid-liquid interface where charge is stored in an electric double layer (EDL). A detailed understanding of the electrostatic capacitance of this EDL is critical for optimizing the energy storage capacity of supercapacitors.[3–5]

Graphene-based electrodes have been identified as a promising candidate for maximizing the specific capacitance at a solid-liquid interface.[6–11] To estimate the theoretical capacity of this

system, a simple (incomplete) analysis uses the specific surface area of graphene (~ 2500 $m^2/g$) and the electrostatic capacitance per unit area of a typical metal/electrolyte interface (~ 0.2 $F/m^2$, see for example Ref. [12]). Multiplying these quantities yields an estimate of 550 F per gram of graphene. To model the system more accurately, however, we must consider both the double-layer capacitance $C_{DL}$ (the electrostatic contribution) and the quantum capacitance of graphene $C_Q$.[8,13–15] Quantum capacitance accounts for the low density of electronic states in graphene (much lower than the density of states of a typical metal). Adding $C_Q$ in series with $C_{DL}$ lowers the total capacitance of the system. The total capacitance of the system may fall even further below initial expectations if $C_{DL}$ is less than 0.2 $F/m^2$. There have been reports of $C_{DL}$ as low as 0.03 $F/m^2$ at the graphene electrolyte interface.[16,17] The goal of our current work is to demonstrate the utility of Hall effect measurements for characterizing and optimizing $C_{DL}$ of graphene/electrolyte interfaces.

In our experiments we study a single layer of graphene and utilize the Hall effect to determine the charge that accumulates at the graphene/electrolyte interface. A Hall voltage, $V_{Hall}$, arises when an electrical current, $I$, moves perpendicular to a magnetic field, $B$. For a p-doped or n-doped two-dimensional material, the Hall voltage is given by $V_{Hall} = IB/en$ or $-IB/ep$ where $e$ is the electron charge and $n$ ($p$) is the sheet density of free electrons (holes) in the material. Thus, $V_{Hall}$ is a direct probe of the carrier concentration on the graphene-side of the EDL. Previous authors have used $V_{Hall}$ to monitor carrier concentration at the graphene-electrolyte interface.[16–20] In these experiments, the total capacitance of the system was not only limited by $C_Q$, but also limited by low values of the double layer capacitance. Hall-effect measurements using polymer electrolyte on graphene found $C_{DL} \leq 0.03$ $F/m^2$,[18,19] similar measurements using an aqueous electrolyte on graphene found $C_{DL} \sim 0.03$ $F/m^2$.[17] Additionally, Hall-effect measurements using ionic liquids on graphene suggest $C_{DL} \leq 0.05$ $F/m^2$ ($C_{DL}$ can be extracted from the data presented in Ref. [16], see SI for our analysis).[16] These previous Hall effect measurements were not focused on supercapacitor applications and, therefore, did not seek to maximize $C_{DL}$ or to demonstrate comparisons between electrolytes. Here we use the Hall effect to compare the performance of different aqueous electrolytes and demonstrate $C_{DL} \geq 0.1$ $F/m^2$.

The Hall effect has important advantages over traditional electrochemical techniques when characterizing the electrostatic capacitance of a solid/electrolyte interface. Traditional

electrochemical approaches (cyclic voltammetry and impedance spectroscopy) do not measure *n* directly, but rather use a time-varying voltage to charge and discharge the EDL.[7–9,14,21,22] An effective capacitance can be inferred from the charging current; however, this current is strongly influenced by the transport of ions in the liquid, and the charging currents are inseparable from Faradaic currents. These issues mean that traditional measurements can yield widely varying results.[21] A second issue is that these traditional methods require an independent measurement of surface area to estimate the charge density. The various techniques that are used to measure surface area can also yield different results.[11] In summary, for 2d materials that are amenable to Hall effect measurements, there are compelling reasons to measures the charge density directly via the Hall effect.

**Methods**

Hall bar devices were fabricated using graphene produced by chemical vapor deposition. A wet transfer process was used to transfer graphene onto an $Si/SiO_2$ substrate. Graphene was patterned and metal leads (5 nm Cr/ 30 nm Au) were deposited using techniques described earlier.[23] The metal electrodes were electrically isolated from the electrolyte by a 70-nm layer of $SiO_2$ that was deposited by e-beam evaporation. A completed device is shown in Figure 1a.

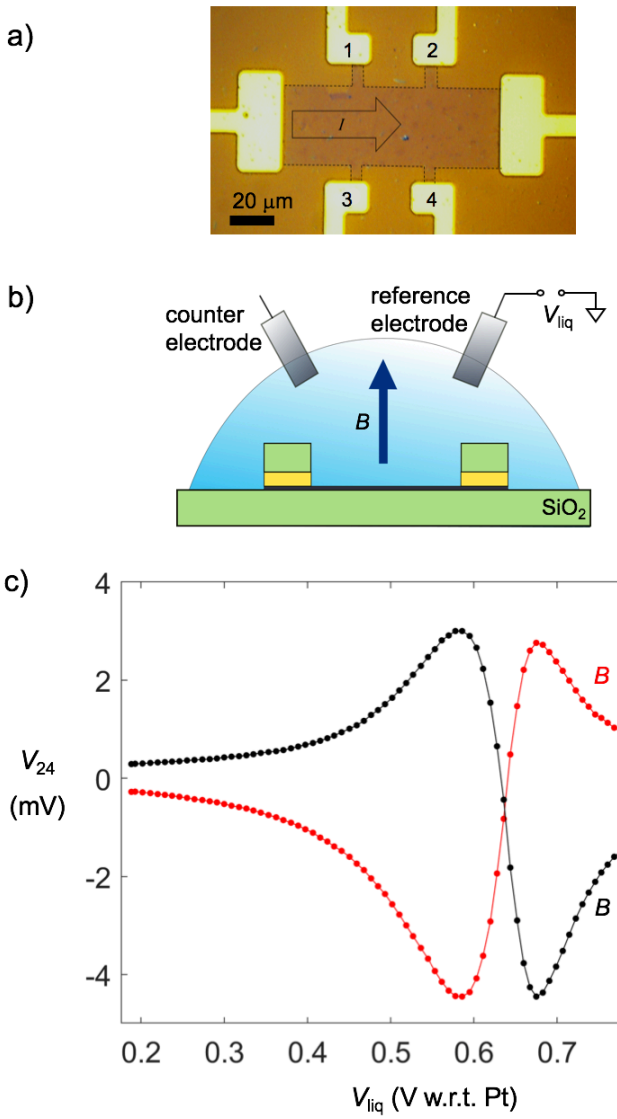


**Figure 1.** a) Optical image of the graphene devices. Dashed black lines show the edge of the patterned graphene. A constant current $I$ = 5 μA flows from the leftmost electrode to the rightmost electrode. The numbered electrodes are used to measure voltage differences. $V_{24}$ is used to detect the Hall voltage, and $V_{12}$ is used to determine the resistivity of graphene. b) Cross-sectional schematic of the device design showing the metal contacts (yellow), the graphene (black), the $SiO_2$ insulation (green), the electrolyte solution and the electrodes submerged in the electrolyte. The blue arrow illustrates the direction of the magnetic field, $B$. c) A typical Hall effect measurement. The electrolyte solution is 600 mM NaCl. Reversing the direction of the magnetic field changes the sign of $V_{24}$. The red and black curves cross at the point of zero charge.

We confirmed the graphene quality by measuring sheet resistance, carrier mobility and the Raman spectrum. We found characteristics that are consistent with high-quality single layer graphene: sheet resistance tunable over one order of magnitude, from 50 Ω/square to 500 Ω/square, a carrier mobility of 3000 $cm^2/V.s$ and a Raman spectra that is characteristic of single layer graphene with a low defect density (see Supporting Information).

The EDL is formed by submerging the graphene device in a liquid electrolyte and applying a voltage difference between the electrolyte and the electrodes that contact the graphene (Fig. 1b). The electrodes contacting the graphene are held at voltages close to ground (there is a small voltage difference across the graphene, ~ 10 mV, required to drive the current for the Hall effect measurement). To control and measure changes in the electrochemical potential of liquid electrolyte, the electrolyte is in contact with both a counter electrode (Pt wire) and quasi-reference electrode (Pt wire). The counter electrode is connected to a voltage source, while the quasi-reference electrode is connected to a high-impedance voltmeter. Changes in the voltmeter reading correspond to changes in the electrochemical potential of the electrolyte solution, $V_{liq}$. We note that changes in the voltmeter reading (the quasi reference electrode) are a fraction of the change in the voltage source (the counter electrode), confirming the need for a counter/reference electrode system.

**Results and Discussion**

Figure 1c shows $V_{24}$ as a function of $V_{liq}$ as $V_{liq}$ is swept in the positive direction at a rate of 6 mV/s. A similar sweep in the negative direction is almost identical, but with a small offset (~ 10 mV) along the $V_{liq}$ axis (see SI). This small amount of hysteresis is expected in the system. To confirm that $V_{24}$ is caused by the Hall effect, we measured with both positive and negative magnetic field and observed the expected change in the polarity of $V_{24}$. When $B > 0$, a positive Hall voltage indicates that electrons are the majority carrier in the graphene, while negative Hall voltage indicates that holes are the majority charge carrier. A cross-over from electrons to holes occurs at $V_{pzc} = 0.64$ V. We identify this cross-over as the point of zero charge (PZC).

Our goal is to determine $C_{DL}$ from Hall voltage data such as Fig. 1c. There are four main steps in our analysis. (1) We remove voltage signals from the $V_{24}$ channel that are uncorrelated to the magnetic field. This is done by calculating $\Delta V_{Hall}$, the change in $V_{24}$ when the magnetic field is switched from +0.5 T to -0.5 T. The blue curve in Figure 2a shows an example of $\Delta V_{Hall}$ as a

function of $V_{liq}$. (2) We quantify the electrostatic disorder in the graphene. It is well-established that electrostatic disorder causes spatial inhomogeneity in the charge density of graphene.[24,25] Importantly for our study, electrostatic disorder changes the relationship between chemical potential, μ, and the spatially-averaged charge density (see Fig. 2b). Additionally, electrostatic disorder determines the range of μ where electrical current is carried by a single carrier type. (3) After identifying the single-carrier regime, we use $\Delta V_{Hall}$ to determine carrier concentration as a function of $V_{liq}$ (see Fig. 3). (4) Finally, we determine $C_{DL}$ by fitting a theoretical curve to the data shown in Fig. 3. Further details about steps (2), (3) and (4) are described below.

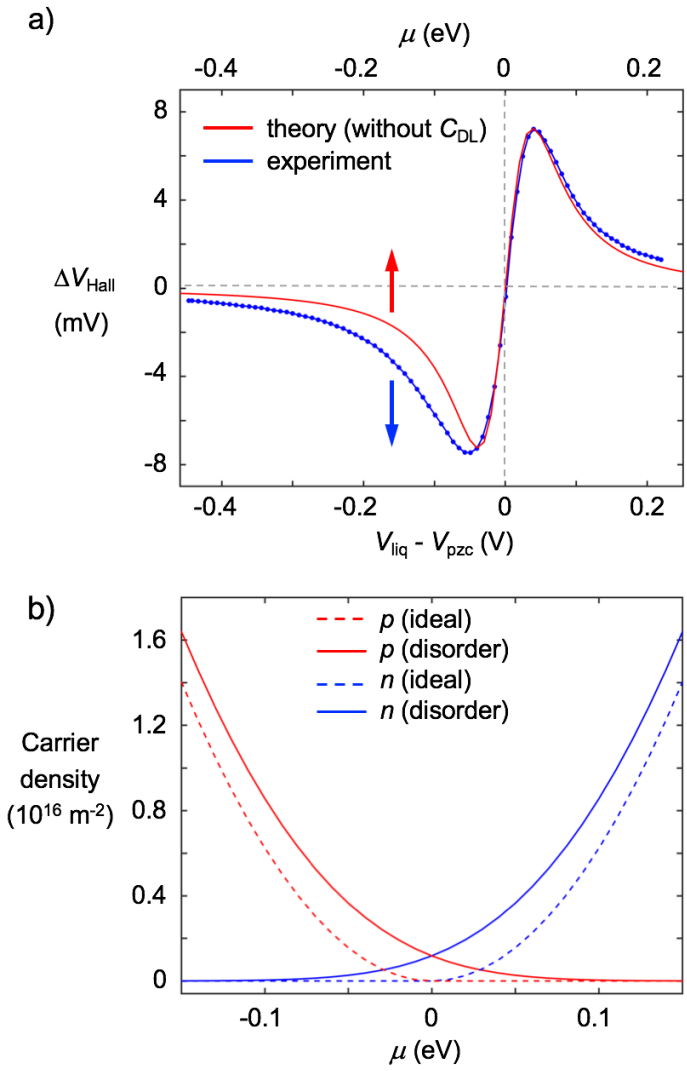


**Figure 2.** a) The expected Hall voltage as a function of chemical potential (red curve) for graphene in the mixed-carrier regime. $\sigma$ = 62 mV, $\Delta B$ = 1 T and $I$ = 5 μA. For comparison, the measured values of $\Delta V_{Hall}$ are plotted with respect to $V_{liq}$ - $V_{pzc}$. b) Carrier concentration as a function of chemical potential for graphene in the mixed-carrier regime (solid lines), compared to ideal graphene at zero temperature (dashed lines).

We first discuss the electrostatic disorder in our graphene sample (step 2 of the analysis). In pristine graphene at zero temperature with no electrostatic disorder, the concentration of free holes is given by

$$p = \begin{cases} \dfrac{\mu^2}{\pi\hbar^2 v_F^2}, & \text{when } \mu < 0 \\ 0, & \text{when } \mu > 0 \end{cases} \qquad (1)$$

where $v_F$ is the Fermi velocity ($\approx 1.1 \times 10^6$ ms$^{-1}$)[26,27] and $\hbar$ is the reduced Planck's constant. A similar expression describes the concentration of free electrons, n. Equation 1 is plotted in Fig. 2b (red dashed line). If electrostatic disorder is introduced to the sample, the spatially-averaged values of *n* and *p* increase (solid lines in Fig. 2b). The spatially-averaged charge density was calculated by assuming that the spread in electrostatic energy is described by a normal distribution with standard deviation σ (see SI for full calculation).[28]

To determine σ for our sample, i.e. to quantify the level of electrostatic disorder, we considered the maximum and minimum values of $\Delta V_{\text{Hall}}$. The mixed-carrier model for the Hall voltage predicts,

$$\Delta V_{\text{Hall}} = \frac{I\Delta B}{e}\frac{n-p}{(n+p)^2}. \qquad (2)$$

Using Eq. 2, together with our model for *n* and *p* (Fig. 2b), we find that σ = 62 mV is consistent with the measured maximum and minimum values of $\Delta V_{\text{Hall}} = \pm 7$ mV.

Equation 2 is plotted on Fig. 2a (red curve plotted with respect to μ) and compared with experimental data (plotted with respect to $V_{\text{liq}} - V_{\text{pzc}}$). Discrepancies between the experimental curve and the theory curve are related to the double layer capacitance, $C_{\text{DL}}$, as discussed below.

To determine capacitance, we must know how *p* (or *n*) changes with respect to $V_{\text{liq}}$ (step 3 of the analysis). It is easiest to determine *p* and *n* in the single-carrier regimes. To define the single-carrier regime for p-doping, we choose the criterion $p > 100n$. This criterion is satisfied when $\mu < -1.5\sigma$ and $p > 1.0 \times 10^{16}$ m$^{-2}$. A similar threshold exists for pure n-doping. In the p-doped single-carrier regime, we have

$$p = \frac{I\Delta B}{e\Delta V_{\text{Hall}}} \qquad \text{when } p > 1.0 \times 10^{16}\ \text{m}^{-2}. \qquad (3)$$

Figure 3a shows *p* as a function of $V_{\text{liq}}$.

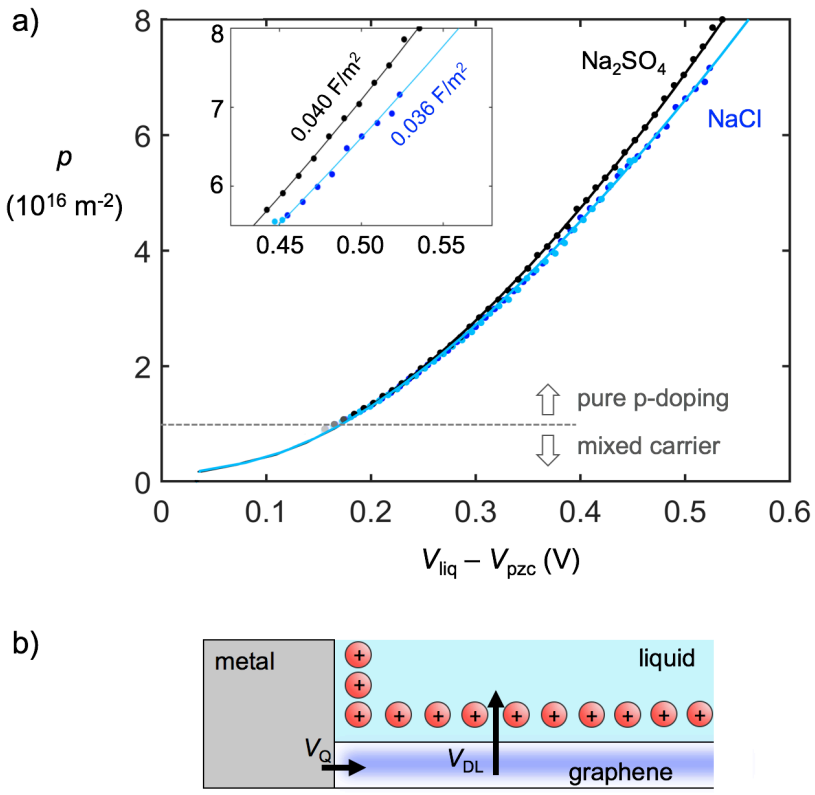


**Figure 3.** a) Sheet density of holes in the graphene, $p$, measured as a function of $|V_{liq} - V_{pzc}|$. The experiment was performed with three different electrolyte solutions, 125 mM NaCl (light blue circles), 600 mM NaCl (dark blue circles), 500 mM $Na_2SO_4$ (black circles). Fit curves (solid blue and black lines) are described in the main text. (Inset) Expanded view of the data high carrier concentration. The curves are labeled with the differential capacitance, $e(\underline{dp}/dV_{liq})$ measured at $p = 7 \times 10^{16}$ m$^2$. b) Schematic showing the EDL formed by negative charge in the graphene (blue cloud) and positive counter ions in solution (red circles). The transfer of charge from the metal electrode to the graphene is driven by an electric field at the metal-graphene interface (voltage drop $V_Q$). The electric field across the EDL corresponds to the voltage drop $V_{DL}$.

For the remainder of this paper, we focus on the measurements taken when the graphene is purely p-doped. In this regime, the EDL is formed by the negatively charged ions in solution (either $Cl^-$ or $SO_4^{2-}$) and the positively charged holes in the graphene. To compare the performance of different ions, we characterized the graphene/electrolyte interface using three different aqueous electrolytes (Fig. 3a). The graphene device was rinsed with deionized water

between each change of electrolyte. There was no measurable difference between the two concentrations of NaCl (125 mM and 600 mM), but a larger $p$ was achieved when using the $Na_2SO_4$ electrolyte. The central result of our paper is this direct comparison of the electrostatic properties of different graphene/electrolyte interfaces.

To complete our analysis, we determined $C_{DL}$ from the charge-voltage relationship (Fig. 3a). To make a first estimate of $C_{DL}$, we used the differential capacitance measurement, $e(dp/dV_{liq})$, together with the expected value of the quantum capacitance, $C_Q = e^2(dp/d\mu)$.[14] The quantum capacitance acts in series with $C_{DL}$ such that

$$\left(e\frac{dp}{dV_{\mathrm{liq}}}\right)^{-1} = \left(C_{\mathrm{Q}}\right)^{-1} + \left(C_{\mathrm{DL}}\right)^{-1}, \qquad (4)$$

In the purely p-doped regime, the quantum capacitance is given by (see SI for derivation)

$$C_Q = \frac{2e^2}{\sqrt{\pi}\hbar v_{\mathrm{F}}}\sqrt{p - p^*}, \qquad \text{where } p^* = \frac{\sigma^2}{\pi\hbar^2 v_F^2}. \qquad (5)$$

For our graphene sample, $p^* = 0.24 \times 10^{16}$ m$^{-2}$. Therefore, at a measured charge density of $p = 7 \times 10^{16}$ m$^{-2}$, we expect $C_Q = 0.066$ F/m$^2$. Using this value of $C_Q$, and the measurements of $e(dp/dV_{liq})$ (Fig. 3 inset) we find that $C_{DL} \approx 0.078$ F/m$^2$ for the NaCl electrolyte and $C_{DL} \approx 0.100$ F/m$^2$ for the $NaSO_4$ electrolyte.

For a more detailed analysis of the charge-voltage curves, we developed a fitting function for Fig. 3 that includes $C_{DL}$ as a fitting parameter. Figure 3b illustrates the two voltage drops, $V_Q$ and $V_{DL}$, that make up the total voltage difference between the metal contact and the electrolyte liquid. The first term, $V_Q = \mu/e$, is the band filling potential (i.e. the cause of quantum capacitance). The second term, $V_{DL}$, is a voltage drop associated with the electric field that extends from the charge carriers in the graphene to the counter ions in the electrolyte. We assume a linear relationship between $V_{DL}$ and $p$ such that $V_{DL} = ep/C_{DL}$. The total voltage drop, in the purely p-doped regime, is then

$$\begin{aligned} \left|V_{\mathrm{liq}} - V_{\mathrm{PZC}}\right| &= \left|V_{\mathrm{Q}}\right| + \left|V_{\mathrm{DL}}\right|, \\ &= \frac{\hbar v_F}{e}\sqrt{\pi(p - p^*)} + \frac{ep}{C_{\mathrm{DL}}}, \qquad \text{where } p > 1.0 \times 10^{16}\ \mathrm{m}^{-2}. \end{aligned} \qquad (6)$$

Equation 6 was used to fit the data shown in Fig. 3a. To achieve the best fit, we set $v_F = 1.2 \times 10^6$ m/s (slightly higher than the typically reported value of $1.1 \times 10^6$ m/s [26,27]). The fitting functions are also offset on the x-axis by 34 mV. The best-fit values of $C_{DL}$ are listed in Table 1.

**Table 1**: Best-fit parameters for the charge-voltage curves shown in Fig. 3.

| | $v_{F,eff}$ (m/s) | $C_{DL}$ (F/m$^2$) |
|---|---|---|
| 125 mM NaCl | $1.2 \times 10^6$ | 0.094 |
| 600 mM NaCl | $1.2 \times 10^6$ | 0.094 |
| 500 mM $Na_2SO_4$ | $1.2 \times 10^6$ | 0.132 |

As expected, the fitting parameter $v_{F,eff}$ is the same for all three electrolytes. We do not expect the choice of electrolyte to affect the $V_Q$ term in Eq. 6. In contrast, the value of $C_{DL}$ clearly changes when we switch from $Cl^-$ to $SO_4^2$. Thus, our Hall effect measurement distinguishes the different EDL structures formed by these anions.

If the graphene sample was ideal, we would expect Eq. 6 to fit exactly (no adjustment to $v_F$, and no offset along the x-axis of Fig. 3a). Imperfections in the graphene may cause deviations from Eq. 6. Defects in the graphene can affect the density of states,[29,30] which would modify the effective Fermi velocity and/or cause an x-axis offset in the charge-voltage curve. Defects can also trap charge in localized states (states that are invisible to the Hall effect measurement), which could cause an x-axis offset. In our graphene sample, the deviation from ideal behavior is relatively minor. Therefore, we have confidence that the $C_{DL}$ values reported in Table 1 are accurate.

It is interesting to consider the relative magnitude of $V_Q$ and $V_{DL}$. For example, when $|V_{liq} - V_{PZC}| = 0.55$ V (the maximum in Fig. 3a), our model predicts that $V_Q$ is larger than $V_{DL}$. This is a useful insight, because supercapacitors are limited by the electrochemical stability of the electrolyte.[3] One can imagine building a pair of electrodes in which only graphene is exposed to the electrolyte (the metal that contacts the graphene would not touch with the electrolyte). In such a system, the total voltage applied between the metal and the liquid ($V_Q + V_{DL}$) could exceed

the stability window of the electrolyte because only $V_{DL}$ drops at the graphene/electrolyte interface.

## Conclusions

We used Hall-effect measurements to perform a comparative study of different electrolytes for graphene supercapacitor applications. We note the key advantage of the Hall technique, namely, the measured signal has a one-to-one correspondence with the charge density in the EDL. In contrast, the results from traditional measurements of capacitance (cyclic voltammetry and impedance spectroscopy) are confounded by effects from electrochemical charge transfer and ion transport. With clean measurements of carrier concentration as a function of applied voltage, we are able to disentangle the separate roles of quantum capacitance and $C_{DL}$. The ability to identify $C_{DL}$ will be increasingly important as supercapacitor electrolytes are developed to withstand higher voltages.[3] Hall-effect measurements, together with other emerging techniques,[31,32] will be a valuable tool for assessing the performance of electrolytes for graphene supercapacitors.

**Supporting Information.** Raman spectrum of the graphene device. Graphene sheet resistance. The Hall-voltage signal measured with forward sweep and backward sweep. Expressions for carrier concentration in the presence of electrostatic disorder. Derivations for Eq. 5 and 6.

## Acknowledgements

We are grateful to Dr. Zhenxing Feng for valuable discussions. Part of this work was conducted at the Northwest Nanotechnology Infrastructure, a National Nanotechnology Coordinated Infrastructure site at Oregon State University which is supported in part by the National Science Foundation (grant NNCI-1542101) and Oregon State University.

**References**


(1) Miller, J.; Simon, P. Electrochemical Capacitors for Energy Management. *Science* **2008**, *321*, 651–652.

(2) Winter, M.; Brodd, R. J. What Are Batteries, Fuel Cells, and Supercapacitors? *Chem. Rev.* **2004**, *104*, 4245–4269.

(3) Béguin, F.; Presser, V.; Balducci, A.; Frackowiak, E. Carbons and Electrolytes for Advanced Supercapacitors. *Adv. Mater.* **2014**, *26*, 2219–2251.

(4) Simon, P.; Gogotsi, Y. Materials for Electrochemical Capacitors. *Nat. Mater.* **2008**, *7*, 845–854.

(5) Kötz, R.; Kötz, R.; Carlen, M.; Carlen, M. Principles and Applications of Electrochemical Capacitors. *Electrochim. Acta* **2000**, *45*, 2483–2498.

(6) Zhu, Y.; Murali, S.; Stoller, M. D.; Ganesh, K. J.; Cai, W.; Ferreira, P. J.; Pirkle, A.; Wallace, R. M.; Cychosz, K. A.; Thommes, M.; *et al*. Carbon-Based Supercapacitors Produced by Activation of Graphene. *Science (80-. ).* **2011**, *332*, 1537–1542.

(7) El-Kady, M. F.; Veronica, S.; Sergey, D.; Richard, B. K. Laser Scribing of High-Performance. *Science (80-. ).* **2012**, *335*, 1326–1330.

(8) Ji, H.; Zhao, X.; Qiao, Z.; Jung, J.; Zhu, Y.; Lu, Y.; Zhang, L. L.; MacDonald, A. H.; Ruoff, R. S. Capacitance of Carbon-Based Electrical Double-Layer Capacitors. *Nat. Commun.* **2014**, *5*, 3317.

(9) Ke, Q.; Wang, J. Graphene-Based Materials for Supercapacitor Electrodes - A Review. *J. Mater.* **2016**, *2*, 37–54.

(10) Cranford, S. W.; Buehler, M. J. Packing Efficiency and Accessible Surface Area of Crumpled Graphene. *Phys. Rev. B* **2011**, *84*, 205451.

(11) Zhang, L.; Zhang, F.; Yang, X.; Long, G.; Wu, Y.; Zhang, T.; Leng, K.; Huang, Y.; Ma, Y.; Yu, A.; *et al*. Porous 3D Graphene-Based Bulk Materials with Exceptional High Surface Area and Excellent Conductivity for Supercapacitors. *Sci Rep* **2013**, *3*, 1408.

(12) Bard, A. J.; Faulkner, L. R. *Electrochemical Methods: Fundamentals and Applications*; Wiley, 2001.

(13) Gerischer, H.; McIntyre, R.; Scherson, D.; Storck, W. Density of the Electronic States of Graphite: Derivation from Differential Capacitance Measurements. *J. Phys. Chem.* **1987**, *91*, 1930–1935.

(14) Xia, J.; Chen, F.; Li, J.; Tao, N. Measurement of the Quantum Capacitance of Graphene. *Nat. Nanotechnol.* **2009**, *4*, 505–509.

(15) Stoller, M. D.; Magnuson, C. W.; Zhu, Y.; Murali, S.; Suk, J. W.; Piner, R.; Ruoff, R. S. Interfacial Capacitance of Single Layer Graphene. *Energy Environ. Sci.* **2011**, *4*, 4685.

(16) Ye, J.; Craciun, M. F.; Koshino, M.; Russo, S.; Inoue, S.; Yuan, H.; Shimotani, H.; Morpurgo, A. F.; Iwasa, Y. Accessing the Transport Properties of Graphene and Its Multilayers at High Carrier Density. *Proc. Natl. Acad. Sci. U. S. A.* **2011**, *108*, 13002–13006.

(17) Dankerl, M.; Hauf, M. V.; Lippert, A.; Hess, L. H.; Birner, S.; Sharp, I. D.; Mahmood, A.; Mallet, P.; Veuillen, J.-Y.; Stutzmann, M.; *et al*. Graphene Solution-Gated Field-Effect Transistor Array for Sensing Applications. *Adv. Funct. Mater.* **2010**, *20*, 3117–3124.

(18) Pachoud, A.; Jaiswal, M.; Ang, P. K.; Loh, K. P.; Özyilmaz, B. Graphene Transport at High Carrier Densities Using a Polymer Electrolyte Gate. *EPL (Europhysics Lett.* **2010**, *92*, 27001.

(19) Efetov, D. K.; Kim, P. Controlling Electron-Phonon Interactions in Graphene at Ultrahigh Carrier Densities. *Phys. Rev. Lett.* **2010**, *105*, 256805.

(20) Bruna, M.; Ott, A. K.; Ijäs, M.; Yoon, D.; Sassi, U.; Ferrari, A. C. Doping Dependence of the Raman Spectrum of Defected Graphene. *ACS Nano* **2014**, *8*, 7432–7441.

(21) Stoller, M. D.; Ruoff, R. S. Best Practice Methods for Determining an Electrode Material's Performance for Ultracapacitors. *Energy Environ. Sci.* **2010**, *3*, 1294.

(22) Crosser, M. S.; Brown, M. A.; McEuen, P. L.; Minot, E. D. Determination of the Thermal Noise Limit of Graphene Biotransistors. *Nano Lett.* **2015**, *15*, 5404–5407.

(23) Brown, M. A.; Crosser, M. S.; Leyden, M. R.; Qi, Y.; Minot, E. D. Measurement of High Carrier Mobility in Graphene in an Aqueous Electrolyte Environment. *Appl. Phys. Lett.* **2016**, *109*, 093104.

(24) Martin, J.; Akerman, N.; Ulbricht, G.; Lohmann, T.; Smet, J. H.; von Klitzing, K.; Yacoby, A. Observation of Electron–Hole Puddles in Graphene Using a Scanning Single-Electron Transistor. *Nat. Phys.* **2008**, *4*, 144–148.

(25) Zhang, Y.; Brar, V. W.; Girit, C.; Zettl, A.; Crommie, M. F. Origin of Spatial Charge Inhomogeneity in Graphene. *Nat. Phys.* **2009**, *5*, 722–726.

(26) Yu, G. L.; Jalil, R.; Belle, B.; Mayorov, A. S.; Blake, P.; Schedin, F.; Morozov, S. V;

Ponomarenko, L. A.; Chiappini, F.; Wiedmann, S.; *et al*. Interaction Phenomena in Graphene Seen through Quantum Capacitance. *Proc. Natl. Acad. Sci. U. S. A.* **2013**, *110*, 3282–3286.

(27) Castro Neto, A. H.; Guinea, F.; Peres, N. M. R.; Novoselov, K. S.; Geim, A. K. The Electronic Properties of Graphene. *Rev. Mod. Phys.* **2009**, *81*, 109–162.

(28) Wojtaszek, M. Graphene: A Two Type Charge Carrier System, University of Groningen, 2009.

(29) Wang, L.; Chen, X.; Zhu, W.; Wang, Y.; Zhu, C.; Wu, Z.; Han, Y.; Zhang, M.; Li, W.; He, Y.; *et al*. Detection of Resonant Impurities in Graphene by Quantum Capacitance Measurement. *Phys. Rev. B* **2014**, *89*, 075410.

(30) Hu, B. Y.-K.; Hwang, E. H.; Das Sarma, S. Density of States of Disordered Graphene. *Phys. Rev. B* **2008**, *78*, 165411.

(31) Kim, C.-H.; Frisbie, C. D. Determination of Quantum Capacitance and Band Filling Potential in Graphene Transistors with Dual Electrochemical and Field-Effect Gates. *J. Phys. Chem. C* **2014**, *118*, 21160–21169.

(32) Froehlicher, G.; Berciaud, S. Raman Spectroscopy of Electrochemically Gated Graphene Transistors: Geometrical Capacitance, Electron-Phonon, Electron-Electron, and Electron-Defect Scattering. *Phys. Rev. B* **2015**, *91*, 205413.